CrossMark

Intrinsic kinetics of CO_2 gasification of a Victorian coal char

Kazi Bayzid Kabir[1,4] · Arash Tahmasebi[2] · Sankar Bhattacharya[1] ·
Jianglong Yu[2,3]

Abstract CO_2 gasification of Victorian (Morwell) brown coal char was studied using a thermogravimetric analyser (TG). Gasification kinetics of demineralised, Ca-loaded, and Fe-loaded Morwell char were also studied. The grain model and random pore model were used to fit the gasification data. The random pore model fitted the experimental data better than the grain model. The activation energy was 189.05 kJ mol^{-1} for the CO_2 gasification of Morwell coal char. With 2 % Ca loading, the activation energy increased to 204.53 kJ mol^{-1} due to lowering of the surface area. However, an order of magnitude increase in the pre-exponential factor indicated an increase in active reaction sites for the 2 % Ca-loaded sample, resulting in a net increase in gasification rate. 5 % Ca loading and 2 % Fe loading proved to be less effective in increasing the gasification rate. Analysis of the TG outlet gas also proved the effectiveness of 2 % Ca loading as a gasification catalyst.

Keywords Victorian brown coal · Morwell coal char · Thermogravimetric analysis · Gasification kinetics

✉ Kazi Bayzid Kabir
    kazibayzid@gmail.com

1   Department of Chemical Engineering, Monash University, Clayton, VIC 3800, Australia

2   School of Chemical Engineering, University of Science and Technology Liaoning, Anshan, Liaoning, China

3   Clean Coal Research, School of Engineering, University of Newcastle, Callaghan, NSW 2308, Australia

4   Present Address: Department of Chemical Engineering, BUET, Dhaka 1000, Bangladesh

Introduction

The objective of gasification is twofold: to convert the non-ash fraction of coal to gas, and to produce gases that preserve, as much as possible, the energy content of the feedstock [1]. Gasification of coal involves two essential steps: devolatilisation (or pyrolysis) of the coal, followed by char gasification. As pyrolysis is a rapid, spontaneous process, char gasification is the rate-limiting step. Char gasification involves reactions between the fixed carbon in coal char and the gasifying agent, usually one or a mixture of oxygen, steam, and carbon dioxide. CO_2 and steam gasification of coal char are an extensively studied research topic because of its importance in power generation and chemical production [2–4].

Char gasification is heterogeneous in nature. The gasification rate depends on various factors such as chemical reactions, mass and heat transfer, impurities in the carbon, and the nature of heat treatment prior to gasification [5]. Non-catalytic gasification is virtually non-existent as all carbon sources contain inherent inorganic impurities, which act as catalysts. Almost all existing metals catalyse the gasification reactions [6].

Victorian brown coals are low in ash. The ash is composed of metallic species (e.g. Ca, Mg, Na) that catalyse gasification and combustion reactions. As a result, Victorian brown coals are highly reactive during gasification. Catalytic gasification is still an emerging technology as it cannot compete economically with non-catalytic gasification processes. Catalytic gasification can only be competitive for a highly reactive coal (for example, Victorian brown coal) if a cheap, active, selective, and recoverable catalyst can be used.

Ohtsuka and Tomita [7] studied steam gasification of Ca-loaded Yallourn (YL) coal at 650 and 700 °C, using six

 Springer

different Ca salts as the precursors. All except $CaSO_4$-loaded coal showed better gasification reactivity. Tomita et al. [8, 9] studied steam gasification of YL coal by nickel impregnation at 500 °C. They used hexammine nickel (II) nitrate solution as the nickel precursor. Ni loading on YL lowered the gasification initiation temperature by 200 °C [9]. Catalytic activity was observed between 4 and 10 mass% and appeared to plateau at 10 mass% Ni loading. The presence of nickel also resulted in in situ desulphurisation by adsorption of sulphur-containing gases by nickel [8]. Takarada et al. [10] studied the reactivity of 34 Ni-loaded coals from 8 different countries and found that the reactivity was strongly dependent on the type of coal, low-rank coals being more reactive.

Catalytic activity of iron was studied using $Fe(NO_3)_3$-, $(NH_4)_3Fe(C_2O_4)_3$-, $FeCl_3$-, and $Fe_2(SO4)_3$-loaded YL coal [11]. Both nitrate and oxalate salts were effective precursors. Following their earlier unsuccessful attempt to use $FeCl_3$ as catalyst precursors, Ohtsuka et al. [12] used a buffer solution (NH_3/NH_4Cl) to precipitate iron at pH 8–9. The chlorine-free, iron-loaded Loy Yang (LY) coal showed a significant improvement in gasification reactivity over the previous study. Urea, $Ca(OH)_2$, and high-temperature hydrolysis were also successfully used for precipitating iron onto LY coal [13], among which $Ca(OH)_2$ precipitated iron acting as the active catalyst even at low loadings of iron (1–5 mass%).

As summarised here, the study of catalytic gasification reported in the literature involves either the use of expensive material (e.g. Ni) or the use of practically non-viable and complex catalyst loading methods. Though these studies provide valuable information on the effectiveness of the catalysts, the efficiency of simple catalyst loading methods and performance of relatively inexpensive metal catalysts should be evaluated.

Kinetics can provide a comparison between the non-catalytic and catalytic gasification of char. Studies on the thermal analysis of Victorian brown coal to determine pyrolysis and combustion kinetics can be found in the open literature [14–19]. However, very few studies reported provided information on the gasification kinetics of Victorian brown coals; those available were summarised by Bhattacharya et al. [20].

Isothermal thermogravimetric studies provide useful information regarding the intrinsic kinetics gasification [21].

The purpose of this study is to determine the intrinsic CO_2 gasification kinetics of a Victorian (Morwell) brown coal char using thermogravimetric (TG) analysis. The effect of inherently present metallic species in Morwell coal was investigated, as well as the effect of loaded catalysts. The two catalysts used, Ca and Fe, were selected for their availability and low cost in comparison with other alternatives.

Materials and methods

Preparation of the coal samples

Victorian (Morwell) brown coal was used for the study. Preparation of the coal sample was done following AS 4264.3-1996 [22]. The as-mined coal sample was air-dried at approximately 35 °C and then pulverised and sieved to different size fractions. The prepared coal fractions were then stored in sample containers.

A three-step washing process was used for coal demineralisation [23]. Initially, the coal sample was washed with a 10 % solution of NaOH. The washing conditions were as follows: 80 °C, 40 min, liquor-to-coal ratio 6 mL g^{-1}. The purpose of the alkali washing step was to convert silica and alumina in the coal to silicate and aluminate forms. Any organic and pyritic sulphur present will also react with NaOH forming precipitates, which are dissolved in subsequent washing steps.

Alkali washing was followed by sulphuric acid leaching. 4 % H_2SO_4 was used with a liquor-to-coal ratio of 2.5 mL g^{-1}. The leaching was carried out at 80 °C for 40 min. Finally, the sample was leached with 20 % nitric acid solution at 80 °C for 40 min, with a liquor-to-coal ratio of 4 mL g^{-1}. The purpose of the acid leaching steps was to dissolve the mineral species as well as the precipitates formed during alkali washing.

Between washing steps, the sample was filtered to remove the spent liquor, washed with demineralised water to remove any trapped solvent, and oven-dried prior to further treatment. The final, demineralised sample was stored in an appropriate sample container. Further details of the washing procedure can be found elsewhere [23].

Catalysts (Ca and Fe) were loaded onto the parent coal by the incipient wetness method [24]. In this method, a small volume of solvent containing nitrate salts of Ca and Fe was added to the coal sample. The volume of solvent was maintained such that it was enough to wet the sample. The slurry was stirred overnight and subsequently dried and stored.

Preparation of char and gasification experiments

A thermogravimetric analyser (TG) (NETZSCH STA 449 F3 Jupiter) was used for char preparation and CO_2 gasification studies. This analyser is designed to operate up to 1250 °C for heating rates between 0.1 and 50 °C min^{-1}.

Alumina crucibles were used for the TG experiments. The dimensions (ID 18 mm, wall thickness 1 mm) of the crucibles were matched to the sample stage. The depth of the crucibles was 2 mm, ensuring that the gas phase could interact with the sample without any bulk diffusion effects. For char

preparation, ca. 10.5 ± 0.5 mg of coal was loaded into the alumina crucible. The sample was heated in 100 mL min^{-1} N$_2$ at 5 °C min^{-1} to 200 °C. When the system temperature reached 200 °C, the heating rate was changed to 10 °C min^{-1} and the temperature ramped to 1000 °C.

In a typical gasification experiment, char prepared according to the above-mentioned method was used. Once the sample temperature reached 1000 °C, it was then cooled to the gasification temperature and stabilised. In a typical run, a mixture of 90 mL min^{-1} of CO$_2$ and 10 mL min^{-1} of N$_2$ was then introduced as the gasifying agent. The sample was exposed to this environment for up to 6 h.

Gasification experiments were carried out at 700, 750, 800, 850, 900, and 1000 °C under 90 % CO$_2$ concentration. To determine the effect of CO$_2$ concentration, additional experiments were carried out at 800 °C under 10, 30, 50, and 70 % CO$_2$ concentrations. Gasification runs under non-isothermal conditions (between 400 and 1100 °C) were also conducted to determine the temperature of initiation of the CO$_2$–char gasification.

Sample characterisation

The proximate analysis of Morwell coal was performed according to the Australian standard AS 2437.4-2002 [25]. Ash composition was determined by ICP/AES following borate fusion and acid dissolution according to AS1038.14.1-2003 [26].

A PerkinElmer 2400 Series II CHNS/O elemental analyser was used for the determination of carbon, hydrogen, nitrogen, and sulphur. The instrument was operated in CHNS mode. A known mass of sample (ca. 1–2 mg) was introduced into the analyser. The sample was combusted in pure oxygen. The resultant combustion gases were separated using frontal chromatography, and a thermal conductivity detector analysed the product gases. Oxygen content was calculated by subtraction.

A Micromeritics Accelerated Surface Area and Porosimetry (ASAP) 2010 analyser was used for the surface area measurements. In a typical run, 100–300 mg of sample was loaded in a sample tube. The sample was degassed at 150 °C, followed by CO$_2$ adsorption at 273.15 K (0 °C).

Results and discussion

The coal properties are shown in Table 1. The as-mined coal is high in moisture, approximately 60 %, which is one of the characteristic features of Victorian brown coals. The proximate and ash analyses are reported on a dry basis. The ultimate analysis is presented on dry ash-free basis.

Gasification reactions are dependent on the rate-controlling step, as the reaction orders, activation energies, and specific reaction rates are affected by it [5]. At lower temperatures, the reaction rate is low enough to make sure that the overall process rate is controlled by chemical processes: chemisorption of the reactants, elementary reactions, and desorption of products. Hence, the reactivity data at lower temperature therefore provide information about intrinsic reaction kinetics. The gasification studies were therefore performed at temperatures between 700 and 1000 °C. Also, a high concentration of CO$_2$ (90 % CO$_2$ in nitrogen) with a shallow, thin-walled crucible was used for these experiments to ensure that no mass transfer limitations were present. Larger particle sizes can also cause diffusion problems and result in a temperature gradient through the particle cross section. The use of small particles (usually <500 μm [27]) is therefore more appropriate for a char–CO$_2$ kinetic study. Kwon et al. [28] showed that the char–CO$_2$ reactivity increased with a decrease in particle size within the range of 180–1000 μm. Here, a much smaller size of coal particles (45–53 μm) was used to prepare the char.

Table 1 Analysis of Morwell coal

Proximate analysis (d.b.)		Ultimate analysis (d.a.f.)		Ash elemental analysis (% oxide in ash)	
Fixed carbon	45.88	Carbon	61.68	SiO$_2$	2.03
Volatile matter	51.82	Hydrogen	4.69	Al$_2$O$_3$	0.97
Ash	2.30	Nitrogen	1.57	Fe$_2$O$_3$	15.28
		Sulphur	0.87	K$_2$O	0.48
		Oxygen	31.09	MgO	19.63
				Na$_2$O	1.26
				CaO	35.49
		Other elements		SO$_3$	24.76
		Chlorine 0.1		P$_2$O$_5$	0.1

Energy content = 26 MJ kg^{-1} (gross dry), 10 MJ kg^{-1} (net wet)
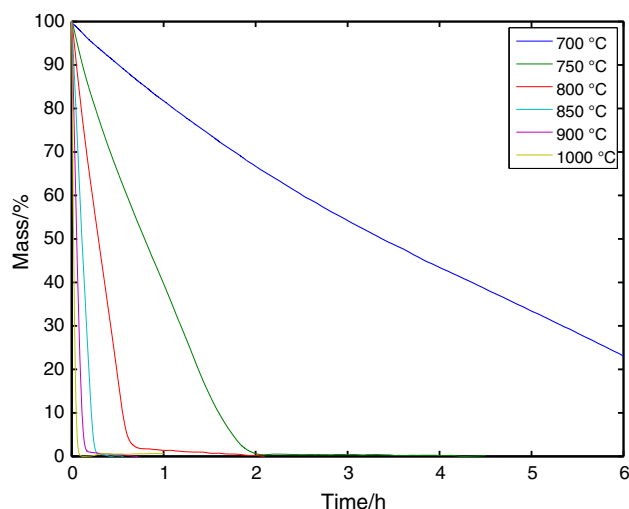
Fig. 1 Mass loss during gasification of Morwell coal char

Changes in mass during CO_2 gasification of Morwell coal char are shown in Fig. 1 on an ash-free basis and only include the char reaction only. The char–CO_2 reaction ($C + CO_2 \rightarrow 2CO$) was very slow at lower temperatures. Complete conversion of char was not achieved at 700 °C, even after 6 h. With a 50 °C increase in temperature, complete conversion of char was achieved in approximately 2 h. The reaction time decreased as the rate increased with an increase in the gasification temperature. At 1000 °C, complete char conversion was achieved in <5 min. The changes in reaction rates from 900 to 1000 °C were not as significant as it was for lower temperatures. This suggests that the rate of reaction above 900 °C was no longer controlled by the chemical reactivity of the solid char alone and that the influence of mass transfer effects was increasing. Hence, only reactivity data up to 900 °C were used in intrinsic reaction kinetics calculations.

The general kinetic expression for char–gas reaction rate can be written as [29]:

$$\frac{dx}{dt} = k(C_g, T)f(x) \tag{1}$$

where x is the char conversion, t is time, and k is the reaction rate, a function of temperature (T) and oxidant concentration (C_g), and $f(x)$ describes the structure factor and dependence on conversion.

Depending on the shape of the extent of reaction against time plot under isothermal conditions, kinetic models involving solid phase can be categorised into three groups: sigmoidal, acceleratory, and deceleratory [30]. For these coal samples, the plots have the same shape as in Fig. 1. Therefore, none of the sigmoidal (e.g. Avrami–Erofeev, Prout–Tompkins) and acceleratory (e.g. exponential, power law) models were considered. As the intrinsic reactivity of a

char sample is mostly dependent on the surface properties, geometrical deceleratory models have proved to be successful in fitting char gasification reactions [31, 32]. Char gasification kinetic models can be classified into three broad groups: volumetric, grain, and random pore models. Among these, volumetric models are too simplified to explain the surface phenomena. Therefore, grain and random pore models were used in this study. The grain model [33], also known as the shrinking core model, assumes an assembly of non-porous grains. The linear form of the GM is [34]:

$$3[1 - (1 - x)^{1/3}] = k_{GM}t \tag{2}$$

where k_{GM} is the reaction rate constant.

The random pore model [35] considers development of pore structure during gasification. As the reaction progresses, the pore becomes larger as carbon is consumed. However, after a certain stage the pores merge, resulting in a net loss of reactive surface area. Hence, a maximum for the reaction rate is observed, which is followed by a declining reaction rate. The linearised form of the RPM is [34]:

$$(2/\psi)[\sqrt{1 - \psi \ln(1 - x)} - 1] = k_{RPM}t \tag{3}$$

The RPM model equation contains two parameters: k_{RPM} is the reaction rate constant and the second parameter, ψ, is a dimensionless structural property.

From the slopes of the plotted experimental results using Eqs. 2 and 3, the reaction rate constants for grain and random pore models, i.e. k_{GM} and k_{RPM}, can be determined. Figure 2 shows the linear forms of both the grain and random pore models for temperatures between 700 and 900 °C. For this study, a range of conversion from 0.05 to 0.70 was used. Five values of reaction rate constants were obtained, one for each temperature.

A constant concentration of 90 % CO_2 in N_2 was used during these experiments. Since the gas concentration remained constant, the rate constants were only dependent on the temperature. This temperature dependence can be expressed using Arrhenius equation:

$$k = k_0 e^{-E_a/RT} \tag{4}$$

where k_0 and E_a are the pre-exponential factor and activation energy, respectively.

Figure 3 shows the Arrhenius plot ($\ln k$ vs T^{-1}) for both models. The kinetic parameters derived from the plots are listed in Table 2. For the random pore model, ψ was used as a fitting parameter and was found to be 1.32. For both models, the activation energy and pre-exponential factor values were similar.

Only experimental data obtained for 700–900 °C were used for the Arrhenius plot and for the determination of the kinetic parameters. The rate constant obtained for 1000 °C

Fig. 2 Plots of the linearised grain and random pore models at different temperatures
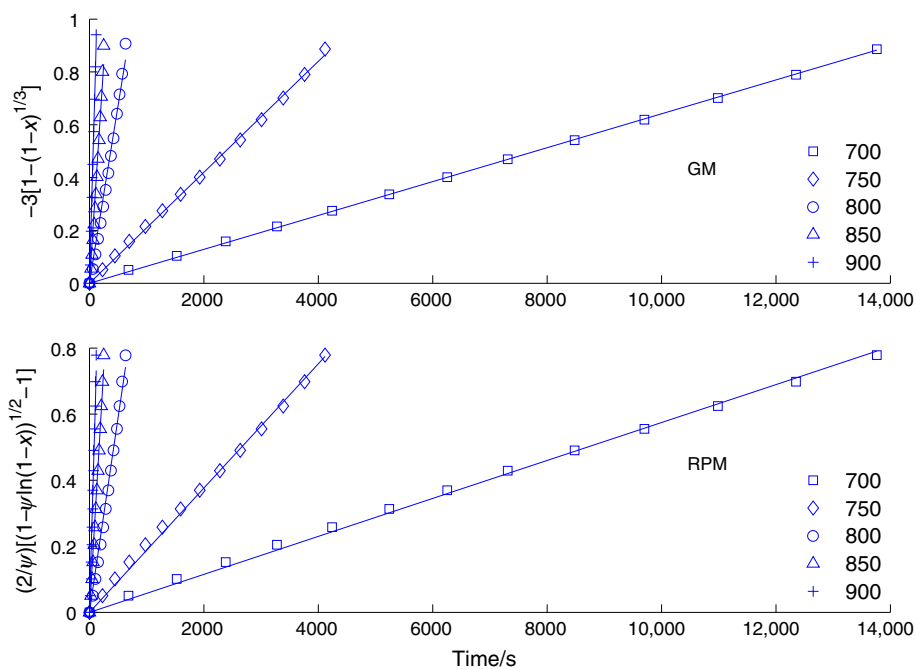
was not used, but is shown in Fig. 3, at the top left corner for both models. This data point does not fit into the Arrhenius plot, indicating that the gasification reaction was no longer chemically controlled. This temperature is therefore within the transition zone between the chemically controlled and diffusion-controlled regimes [5], where the gasification rate is jointly controlled by both chemical reaction at the surface and mass transfer in the pores.

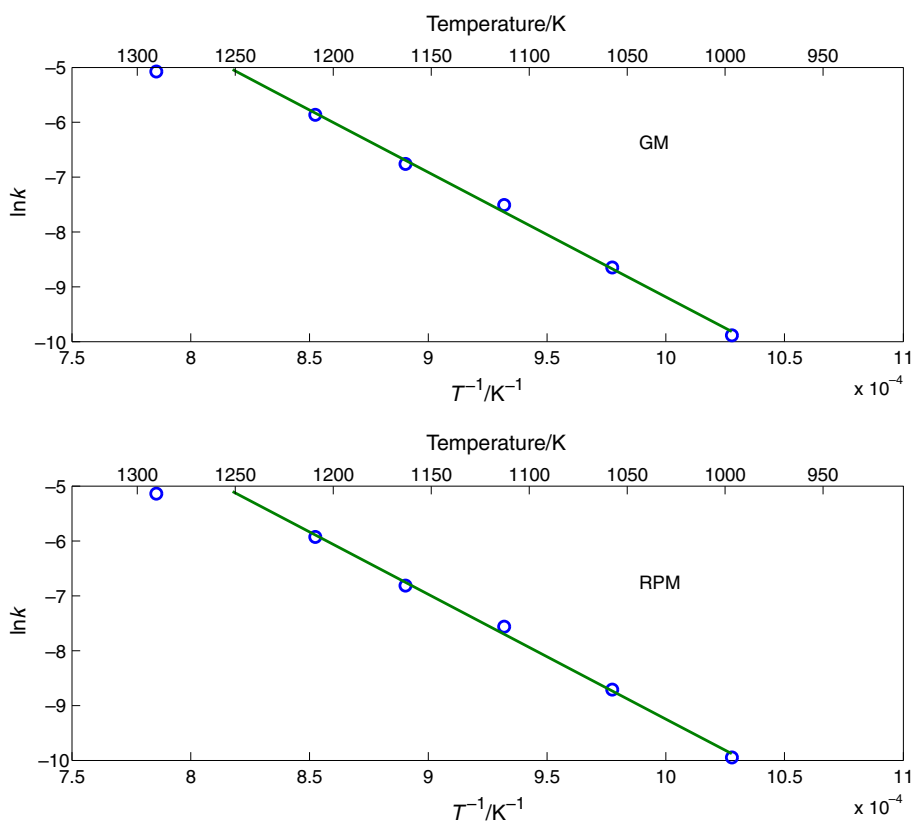**Fig. 3** Arrhenius plots for grain and random pore models

Table 2 Grain and random pore model parameters for Morwell coal char

	E_a/kJ mol^{-1}	k_0/s^{-1}	ψ	R^2
Grain model	188.99	7.67×10^5	–	0.9822
Random pore model	189.05	7.23×10^5	1.32	0.9831

To determine the validity of the models, Eqs. 2 and 3 were used to predict the conversion over time and compared with the experimental data. A comparison of the experimental and predicted values is shown in Fig. 4. Both models showed good prediction of the experimental data, with increasing deviation at higher conversions. At 700 °C, both models slightly overpredicted the conversion. At higher temperatures, the models underpredicted the conversion. Coefficients of determination, R^2, are shown in Table 2. Though both models gave acceptable performance, the random pore model predicted the conversion data slightly better than the grain model.

To determine the effect of CO_2 concentration, gasification experiments were carried out at CO_2 concentrations of 10, 30, 50, 70, and 90 %. If the order of the reaction is n with respect to CO_2 concentration, the concentration dependence can be described as:

$$k = k' C_{H_2O}^n \qquad (5)$$

The reaction order with respect to CO_2 concentration can be determined from the slope of the straight lines. Plots for grain and random pore models are shown in Fig. 5. The

slopes of these lines are identical, and thus n for both modes was 0.34.

There are several postulated mechanisms for carbon–CO_2 reaction [5, 36, 37]. Each mechanism suggests that the reaction order with respect to CO_2 should be in between 0 and 1. The order may be anywhere within this range and varies with temperature, pressure, nature of purity of the carbon, and geometric dimensions of the sample [5]. Therefore, an order of 0.34 is consistent with the previous findings. The order of the gasification reaction depends on the relationship between the fraction of the surface covered by the carbon–oxygen complex and change in the pressure of the reacting gas. A lower order of the reaction indicates that the product of the pressure and the rate constant for the formation of the surface complex is large compared to the rate constant for the conversion of the surface complexes to the product. A lower reaction order therefore indicates that the reaction is controlled by the chemical processes rather than diffusion of the reacting gas.

Alkali (K, Na) and alkaline earth (Ca, Mg) metals as well as transition (Fe, Ni) metals are known to catalyse the gasification of carbon by CO_2 [38]. Morwell coal has high inherent calcium, magnesium, and iron content. It also contains lower amounts of sodium and potassium. The presence of these metal species in Morwell coal makes it one of the most reactive coals [10].

Acid-washed coal loaded with alkali and alkaline earth metals as well as iron and nickel has been studied to determine the effect of their individual loading [39].

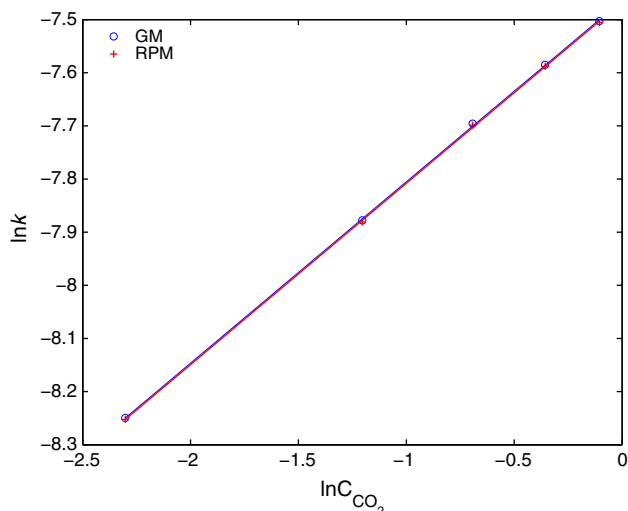**Fig. 4** Comparison between the experimental and predicted conversion
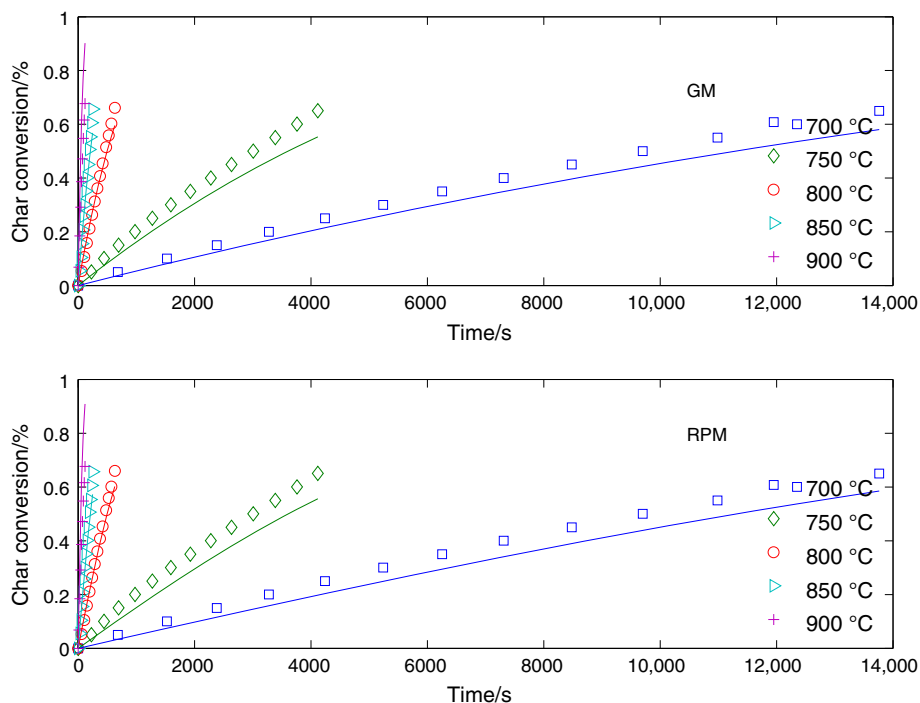
Fig. 5 Dependence of reaction rate on CO$_2$ concentrations

Though these studies provided important information regarding the catalytic effect and kinetics, demineralisation followed by catalyst loading is impractical as the process is tedious and requires disposal of acidic wastes.

To study the effect of inherently present metals on the gasification, Morwell coal was demineralised using a three-step washing method [23]. In addition to the demineralised coal (DEM), few more catalyst-loaded samples were prepared. The current study focuses more on the practical side of catalytic gasification. Therefore, catalyst loading was done on the coal sample as it is.

For catalyst loading, two different methods were applied: water soaking and physical mixing. In water soaking, a salt solution was used to load the sample using incipient wetness method. Physical mixing involved mixing the dry salt with the coal. While physical mixing has the benefit of ease of operation, the water soaking method is also considered viable if the salt is mixed with water.

Of the three groups of gasification catalysts, alkali metals were not considered for this study. Salts of alkali metals are highly volatile and retention of these species is very low as the coal temperature exceeds 700 °C [40]. Calcium and iron were selected from the alkaline earth and transition metal groups, respectively. Both calcium and iron are relatively inexpensive and readily available in comparison with the other potentially catalytic elements in their respective groups. Nitrate salts were used for the study. For 2 % extra calcium loading, both water soaking (CAL2) and physical mixing (CAL2PM) loading methods were used. A 5 % Ca-loaded (CAL5) sample was prepared by water soaking. For iron loading, 2 and 5 % in excess of inherent iron content, the water soaking method was used (FE2, FE5).

Several gasification runs were conducted at non-isothermal (dynamic) condition. Chars were prepared at 1000 °C in the TG. The samples were then cooled in situ to 400 °C before introducing the gasifying agent, 90 % CO$_2$ in nitrogen. In contrast to the isothermal runs, in this case the temperature was then ramped to 1100 °C at a heating rate of 10 °C min^{-1}.

The purpose of these experiments was to determine the temperature of initiation of the gasification (T_S). Also, the temperature of maximum reactivity (T_{MAX}) and the temperature of complete conversion (T_E) were determined, and the results are shown in Table 3. DTG curves, shown in Fig. 6, were used to find these temperatures.

From Table 3, it can be concluded that the addition of calcium and iron did not affect any of the characteristic temperatures obtained from the DTG curves. The sample without any mineral, i.e. DEM, showed a 65 °C increase in temperature. The removal of alkaline earth metal species has caused this variation, as these metals are known to reduce the gasification temperature by up to 150 °C [41]. For DEM, both T_{MAX} and T_E also shifted towards the higher end. This result is a clear indication of the catalytic effect of the inherently present minerals in Morwell brown coal. Among the physically mixed and water-soaked 2 % Ca-loaded samples, the water-soaked sample showed slightly better performance due to better dispersion of the calcium species during the water soaking method.

To understand the effect of demineralisation and loading with calcium and iron, isothermal gasification experiments were carried out in a TG at temperatures between 700 and 1000 °C, using 90 % CO$_2$ in N$_2$ as the gasifying agent. Experimental data were then fitted to random pore model to find the reaction rate constant at different temperatures. The corresponding Arrhenius plots are shown in Fig. 7. The results show that the DEM sample was the least reactive of all these samples. FE2 showed slightly better performance than the Morwell coal at lower temperatures. However, the differences in the rate constants diminished at higher temperatures. CAL2 showed better performance than FE2 and FE5 over this temperature range.

At temperatures above about 1000 °C, CO$_2$ gasification of char is no longer controlled by chemical processes

Table 3 Characteristic temperatures from the DTG curves under non-isothermal condition

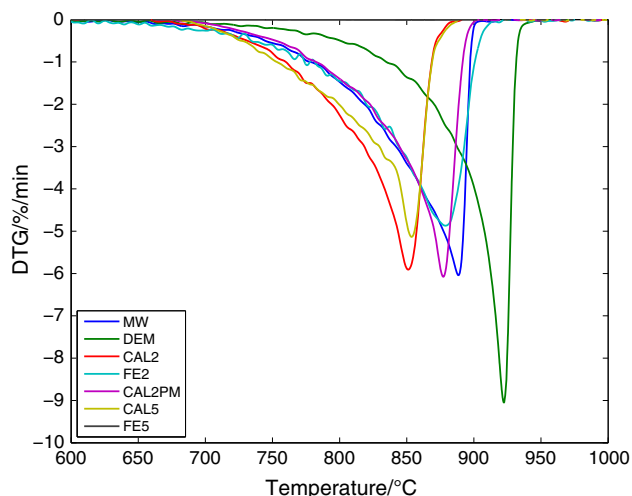| Sample	T_S/°C	T_{MAX}/°C	T_E/°C
Morwell (parent coal char)	658	888	903
DEM	723	923	938
CAL2	658	850	892
CAL2PM	658	873	900
CAL5	658	853	888
FE2	653	877	915
FE5	658	862	900

Fig. 6 DTG plots of non-isothermal gasification of coal chars

alone. Though rate constants at 1000 °C are shown in Fig. 7 (circled at the top left), they were not used for the determination of kinetic parameters. It can be seen from the plot that the data points at 1000 °C are clustered together, indicating that the rate is almost independent of surface chemical reactions. The data points grouping together also indicate that the Arrhenius plots at higher temperature are converging and gradually approaching the isokinetic point. One major conclusion can be drawn from this result: catalytic gasification for Morwell coal is only beneficial if the gasification temperature is maintained at or below 900 °C.

Kinetic parameters obtained from the Arrhenius plots shown in Fig. 7 are listed in Table 4. The CO_2 surface area determined for the samples is also shown in the first column of Table 4. The activation energy was lowest for the Morwell coal. For calcium and iron loading, the activation energies were similar and slightly higher than the Morwell
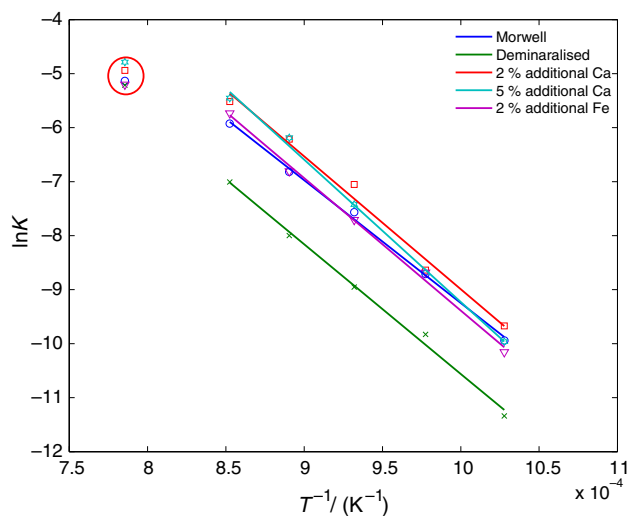

Fig. 7 Arrhenius plots for demineralised and catalyst-loaded samples

coal. For the alkaline earth or transition metals-loaded coal samples, a net decrease in surface area was observed, as some of the pores are obscured by metal atoms, making them inaccessible to the gaseous species. Although surface area was lower for CAL2 and FE2, the catalytic effect of Ca and Fe increased the numbers of active sites for the reaction as indicated by the higher pre-exponential factor. For CAL2, the increase was one order of magnitude and hence this sample showed better catalytic activity. DEM was free of inherently present minerals and therefore had a larger surface area than the parent coal. The pre-exponential factor for the DEM sample also indicates that the reaction sites are less than that for the parent coal. This indicates that the absence of the catalytic species is the major contributing factors to the lower reactivity of this sample. For the CAL5 sample, the pre-exponential factor was higher than that for the CAL2 sample. However, the measured CAL5 surface area was 60 % of that of the parent coal, which resulted in a decrease in specific rate constant at lower temperature. At 850 and 900 °C, it was similar to that of CAL2. The activation energy was 222.28 kJ mol^{-1} for this sample.

Though the Morwell parent coal is already rich in calcium, the addition of 2 and 5 % calcium to the coal improved the gasification reactivity. However, with 5 % loading there was no improvement in the reactivity compared to 2 % loading.

Upon heating, calcium nitrate decomposes to calcium oxide, giving up two moles of NO_2 and half mole of O_2. The decomposition begins at 500 °C [42].

$$Ca(NO_3)_2 \rightarrow CaO + 2NO_2 + 1/2O_2 \qquad (R\text{-}1)$$
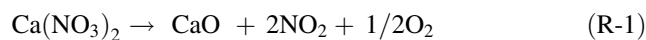
CaO formed from calcium nitrate is amorphous in nature [7] and therefore ensures fine dispersion of calcium throughout the coal sample.

During pyrolysis of CAL2 and CAL5, the introduced nitrate salt decomposed into calcium oxide. When CO_2 was introduced into the system, calcium oxide reacted with CO_2 forming $CaCO_3$. This carbonate then reacted with carbon to form CO and calcium oxide again. The overall mechanism can be summarised as [43]:

$$CaO + CO_2 \rightarrow CaCO_3 \qquad (R\text{-}2)$$

$$CaCO_3 + C \rightarrow CaO + 2CO \qquad (R\text{-}3)$$

giving the overall gasification reaction:

$$C + CO_2 \rightarrow 2CO \qquad (R\text{-}4)$$

Since $CaCO_3$ is one of the intermediates, it may also be considered as a potential calcium source. However, direct decomposition of $CaCO_3$ gives CaO with slightly higher crystallite size than that of nitrate [7]. Therefore, the reactivity is expected to be lower than for nitrate salt-
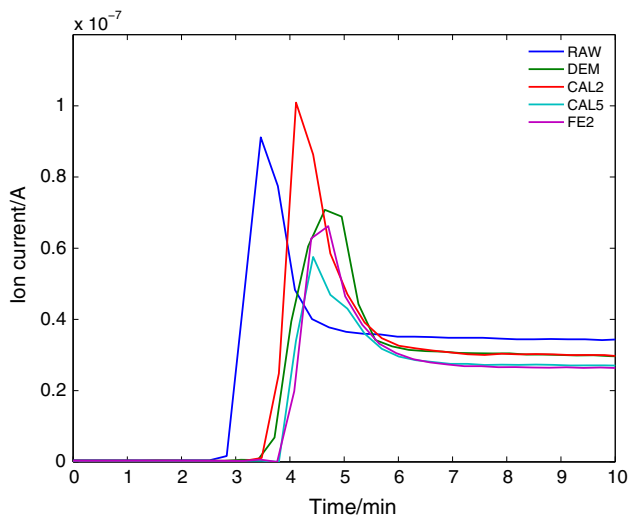
Table 4 Kinetic parameters for coal char gasification according to random pore

Sample (CO_2 surface area/ m^2 g^{-1})	E_a/ kJ mol^{-1}	k_0/s^{-1}	Ψ
MW (190.90)	189.05	7.25×10^5	1.32
DEM (218.25)	199.60	6.93×10^5	10.02
CAL2 (160.31)	204.53	6.02×10^6	0.91
CAL5 (113.25	222.28	4.38×10^7	0.68
FE2 (173.90)	202.92	2.99×10^6	3.3

derived CaO. However, even considering its potentially lower catalytic value, $CaCO_3$ may be a preferable option compared to $Ca(NO_3)_2$, as carbonates are widely available and relatively inexpensive.

The yield of CO (arbitrary units) for different samples was recorded using mass spectroscopy and is shown in Fig. 8. For the MS measurements, gasification experiments were performed at 1000 °C, with argon as the carrier gas. There was a transport delay of 2–3 min from the TG to the MS detector. The yield of CO is given by area under the peak and increased from the MW to the CAL2 sample. The reading for the CO then flattened out which indicates exhaustion of carbon in the char sample. The peak height of the FE2 and CAL5 samples were smaller than of the DEM sample, all of which are significantly lower than of the CAL2 sample.

The maximum peak height of CO in Fig. 8 can be considered to represent the CO production rate if char supply is non-exhaustive. Therefore, these peaks give an indication of gasification rate in a continuous feed process. The results suggest that 2 % Ca loading on Morwell char would improve the continuous gasification rate compared to the MW parent coal char.

Addition of 2 % Fe did not show better reactivity. The reaction at lower temperature required longer time and resulted in complete oxidation. Therefore, at these temperatures the Fe-loaded sample showed lower reactivity than the parent coal. Several forms of iron are known to be inactive for C–CO_2 reaction. Both haematite and magnetite are not active catalysts for this reaction [44]. Under the experimental conditions used in this study, any other forms of iron (e.g. Fe and wustite) would be oxidised by CO_2 and hence form inactive phases [44].

Conclusions

The intrinsic CO_2 gasification kinetics of Morwell coal char were studied using the grain and random pore models. Both models adequately predict the gasification behaviour of the Morwell coal char, and the random pore model fitted the experimental data slightly better than the grain model. The activation energy of CO_2–char reaction determined by the random pore model was 189.05 kJ mol^{-1}.

The removal of mineral matters from coal prior to gasification lowered the gasification rate due to the absence of the minerals' catalytic effect. Ca loading is proved to be effective in increasing char reactivity through the creation of more reaction sites. 2 % loading of Ca on Morwell coal proved to be most effective. Iron loading on the coal sample did not show any improvement in gasification rate. The observed kinetic data were complemented by the mass spectroscopy on the TG outlet gas.

Fig. 8 MS of TG outlet gas, recorded for mass = 28 (CO)

References

1. Bell DA, Towler BF. Coal gasification and its application. Boston: William Andrew Publishing; 2011.
2. Tomaszewicz M, Łabojko G, Tomaszewicz G, Kotyczka-Morańska M. The kinetics of CO2 gasification of coal chars. J Therm Anal Calorim. 2013;113(3):1327–35. doi:10.1007/s10973-013-2961-2.
3. Chmielniak T, Sciazko M, Tomaszewicz G, Tomaszewicz M. Pressurized CO2-enhanced gasification of coal. J Therm Anal Calorim. 2014;117(3):1479–88. doi:10.1007/s10973-014-3879-z.
4. Zhao H, Cao Y, Orndorff W, Pan W-P. Gasification characteristics of coal char under CO2 atmosphere. J Therm Anal Calorim. 2014;116(3):1267–72. doi:10.1007/s10973-013-3627-9.
5. Walker PL Jr, Rusinko F Jr, Austin LG. Gas reactions of carbon. In: Selwood DD, Eley PWS, Paul BW, editors. Advances in catalysis. New York: Academic Press; 1959. p. 133–221.
6. Radovic LR. Catalysis in coal and carbon gasification. Handbook of heterogeneous catalysis. Hoboken: Wiley; 2008.
7. Ohtsuka Y, Tomita A. Calcium catalysed steam gasification of Yallourn brown coal. Fuel. 1986;65(12):1653–7. doi:10.1016/0016-2361(86)90264-4.
8. Tomita A, Ohtsuka Y, Tamai Y. Low temperature gasification of brown coals catalysed by nickel. Fuel. 1983;62(2):150–4. doi:10.1016/0016-2361(83)90187-4.

9. Tomita A, Tamai Y. Low-temperature gasification of Yallourn coal catalysed by nickel. Fuel. 1981;60(10):992–4. doi:10.1016/0016-2361(81)90099-5.

10. Takarada T, Tamai Y, Tomita A. Reactivities of 34 coals under steam gasification. Fuel. 1985;64(10):1438–42. doi:10.1016/0016-2361(85)90347-3.

11. Ohtsuka Y, Tamai Y, Tomita A. Iron-catalyzed gasification of brown coal at low temperatures. Energ Fuels. 1987;1(1):32–6. doi:10.1021/ef00001a006.

12. Ohtsuka Y, Asami K. Steam gasification of low-rank coals with a chlorine-free iron catalyst from ferric chloride. Ind Eng Chem Res. 1991;30(8):1921–6. doi:10.1021/ie00056a038.

13. Asami K, Ohtsuka Y. Highly active iron catalysts from ferric chloride for the steam gasification of brown coal. Ind Eng Chem Res. 1993;32(8):1631–6. doi:10.1021/ie00020a014.

14. Ma S, Hill JO, Heng S. A thermal analysis study of the pyrolysis of Victorian brown coal. J Therm Anal. 1989;35(3):977–88. doi:10.1007/BF02057254.

15. Ma S, Hill JO, Heng S. A thermal analysis study of the combustion characteristics of Victorian brown coals. J Therm Anal. 1989;35(6):1985–96. doi:10.1007/BF01911681.

16. Ma S, Hill JO, Heng S. A thermal analysis study of the oxidation of brown coal chars. J Therm Anal. 1989;35(5):1611–9. doi:10.1007/BF01912936.

17. Hill JO, Ma S, Heng S. Thermal analysis of Australian coals—a short review. J Therm Anal. 1989;35(6):2009–24. doi:10.1007/BF01911683.

18. Ma S, Hill JO, Heng S. A kinetic analysis of the pyrolysis of some australian coals by non-isothermal thermogravimetry. J Therm Anal. 1991;37(6):1161–77. doi:10.1007/BF01913852.

19. Yeasmin H. Measurements and modelling of kinetics of devolatilisation of low-rank coal at elevated pressures and temperatures. Clayton: Monash University; 1998.

20. Bhattacharya S, Kabir KB, Hein K. Dimethyl ether synthesis from Victorian brown coal through gasification—current status, and research and development needs. Prog Energy Combust Sci. 2013;39(6):577–605. doi:10.1016/j.pecs.2013.06.003.

21. Liu L, Liu Q, Cao Y, Pan W-P. The isothermal studies of char-CO2 gasification using the high-pressure thermo-gravimetric method. J Therm Anal Calorim. 2015;120(3):1877–82. doi:10.1007/s10973-015-4476-5.

22. Standards Australia. Coal and coke—sampling, part 3: lower rank coal—sampling procedures (AS 4264.3-1996). Sydney: Standards Australia; 1996.

23. Yang RT, Das SK, Tsai BMC. Coal demineralization using sodium hydroxide and acid solutions. Fuel. 1985;64(6):735–42. doi:10.1016/0016-2361(85)90002-X.

24. Augustine RL. Heterogeneous catalysis for the synthetic chemist. New York: Marcel Dekker; 1996.

25. Standards Australia. Methods for the analysis and testing of low rank coal and its char (AS 2437.4-2002). Sydney: Standards Australia; 2002.

26. Standards Australia. Coal and coke—analysis and testing—higher rank coal ash and coke ash—major and minor elements—borate fusion/flame atomic absorption spectrometric method (AS 1038.14.1-2003). Sydney: Standards Australia; 2003.

27. Wen CY, Dutta S. Solid–gas reactions in coal conversion processes. Coal processing technology, vol. 4. New York: AIChE; 1978. p. 40–51.

28. Kwon T-W, Kim SD, Fung DPC. Reaction kinetics of char—CO_2 gasification. Fuel. 1988;67(4):530–5.

29. Lu GQ, Do DD. Comparison of structural models for high-ash char gasification. Carbon. 1994;32(2):247–63. doi:10.1016/0008-6223(94)90188-0.

30. Xiong C. Use of simplified chemical kinetics in simulation of combustion and explosions. Ann Arbor: The University of Utah; 2007.

31. Irfan MF, Usman MR, Kusakabe K. Coal gasification in CO2 atmosphere and its kinetics since 1948: a brief review. Energy. 2011;36(1):12–40. doi:10.1016/j.energy.2010.10.034.

32. Molina A, Mondragón F. Reactivity of coal gasification with steam and CO2. Fuel. 1998;77(15):1831–9. doi:10.1016/S0016-2361(98)00123-9.

33. Szekely J, Evans JW. A structural model for gas–solid reactions with a moving boundary. Chem Eng Sci. 1970;25(6):1091–107. doi:10.1016/0009-2509(70)85053-9.

34. Fermoso J, Arias B, Pevida C, Plaza MG, Rubiera F, Pis JJ. Kinetic models comparison for steam gasification of different nature fuel chars. J Therm Anal Calorim. 2008;91(3):779–86. doi:10.1007/s10973-007-8623-5.

35. Bhatia SK, Perlmutter DD. A random pore model for fluid-solid reactions: I. Isothermal, kinetic control. AIChE J. 1980;26(3):379–86. doi:10.1002/aic.690260308.

36. Gadsby J, Long FJ, Sleightholm P, Sykes KW. The mechanism of the carbon dioxide-carbon reaction. Proc R Soc A. 1034;1948(193):357–76.

37. Reif AE. The mechanism of the carbon dioxide-carbon reaction. J Phys Chem. 1952;56(6):785–8. doi:10.1021/j150498a033.

38. Nishiyama Y. Catalytic gasification of coals—features and possibilities. Fuel Process Technol. 1991;29(1–2):31–42. doi:10.1016/0378-3820(91)90015-5.

39. Li C-Z. Some recent advances in the understanding of the pyrolysis and gasification behaviour of Victorian brown coal. Fuel. 2007;86(12–13):1664–83. doi:10.1016/j.fuel.2007.01.008.

40. Ji Hayashi, Takahashi H, Iwatsuki M, Essaki K, Tsutsumi A, Chiba T. Rapid conversion of tar and char from pyrolysis of a brown coal by reactions with steam in a drop-tube reactor. Fuel. 2000;79(3–4):439–47. doi:10.1016/S0016-2361(99)00179-9.

41. Ohtsuka Y, Asami K. Steam gasification of coals with calcium hydroxide. Energ Fuels. 1995;9(6):1038–42. doi:10.1021/ef00054a016.

42. Laue W, Thiemann M, Scheibler E, Wiegand KW. Nitrates and nitrites. Ullmann's encyclopedia of industrial chemistry. Weinheim: Wiley; 2002. p. 149–76.

43. McKee DW. Catalytic effects of alkaline earth carbonates in the carbon-carbon dioxide reaction. Fuel. 1980;59(5):308–14. doi:10.1016/0016-2361(80)90215-X.

44. Walker PL Jr, Shelef M, Anderson RA. Catalysis of carbon gasification. In: Walker Jr PL, editor. Chemistry and physics of Carbon, vol. 4. New York: Marcel Dekker; 1968. p. 287–383.